Nano Hexapod - Optimal Geometry

Dehaeze Thomas

March 30, 2025

Contents

- In the conceptual design phase, the geometry of the Stewart platform was chosen arbitrarily and not optimized
- In the detail design phase, we want to see if the geometry can be optimized to improve the overall performances
- Optimization criteria: mobility, stiffness, dynamical decoupling, more performance / bandwidth

Outline:

- Review of Stewart platform (Section 1) Geometry, Actuators, Sensors, Joints
- Effect of geometry on the Stewart platform characteristics (Section 2)
- Cubic configuration: benefits? (Section **??**)
- Obtained geometry for the nano hexapod (Section **??**)

1 Review of Stewart platforms

- As was explained in the conceptual phase, Stewart platform have the following key elements:
  - Two plates connected by six struts
  - Each strut is composed of:
    - a flexible joint at each end
    - an actuator
    - one or several sensors
- The exact geometry (i.e. position of joints and orientation of the struts) can be chosen freely depending on the application.
- This results in many different designs found in the literature.
- The focus is here made on Stewart platforms for nano-positioning and vibration control. Long stroke stewart platforms are not considered here as their design impose other challenges. Some Stewart platforms found in the literature are listed in Table 1.1
- All presented Stewart platforms are using flexible joints, as it is a prerequisites for nano-positioning capabilities.
- Most of stewart platforms are using voice coil actuators or piezoelectric actuators. The actuators used for the Stewart platform will be chosen in the next section.
- Depending on the application, various sensors are integrated in the struts or on the plates. The choice of sensor for the nano-hexapod will be described in the next section.
- There are two categories of Stewart platform geometry:
  - Cubic architecture (Figure 1.1). Struts are positioned along 6 sides of a cubic (and are therefore orthogonal to each other). Such specific architecture has some special properties that will be studied in Section **??**.
  - Non-cubic architecture (Figure 1.2)

Conclusion:

- Various Stewart platform designs:
  - geometry, sizes, orientation of struts

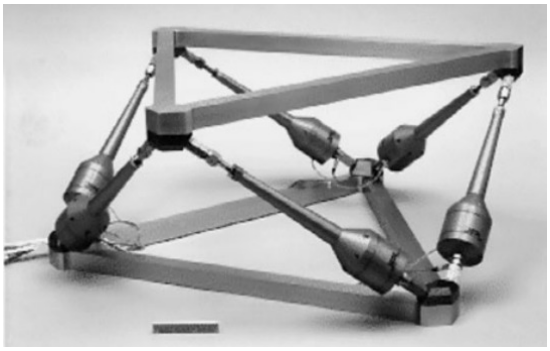

(a) California Institute of Technology - USA

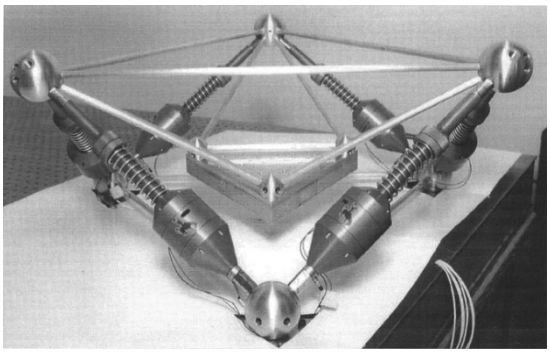

(b) University of Wyoming - USA

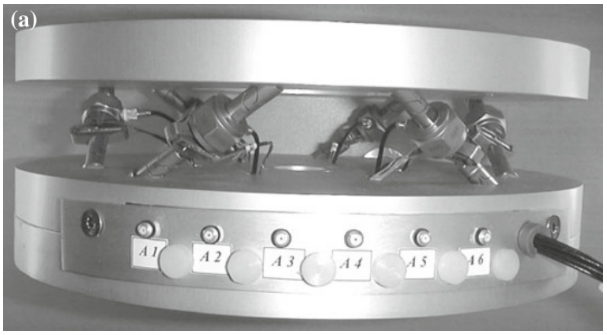

(c) ULB - Belgium

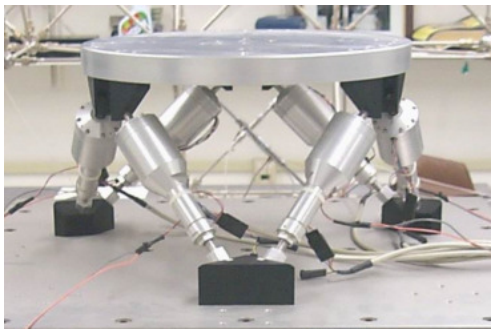

(d) Naval Postgraduate School - USA

Figure 1.1: Some examples of developped Stewart platform with Cubic geometry. (a), (b), (c), (d)

Table 1.1: Examples of Stewart platform developed. When not specifically indicated, sensors are included in the struts. All presented Stewart platforms are using flexible joints. The table is ordered by appearance in the literature

	Geometry	Actuators	Sensors	Reference
	Cubic	Magnetostrictive	Force, Accelerometers	[1]–[3]
Figure 1.1a	Cubic	Voice Coil (0.5 mm)	Force	[4], [5]
	Cubic	Voice Coil (10 mm)	Force, LVDT, Geophones	[6]–[8]
Figure 1.1b	Cubic	Voice Coil	Force	[9]–[13]
	Cubic	Piezoelectric (25 μm)	Force	[14]
Figure 1.1c	Cubic	APA (50 μm)	Force	[15]
Figure 1.2a	Non-Cubic	Voice Coil	Accelerometers	[16]
	Cubic	Voice Coil	Force	[17], [18]
Figure 1.1d	Cubic	Piezoelectric (50 μm)	Geophone	[19]
	Non-Cubic	Piezoelectric (16 μm)	Eddy Current	[20]
	Cubic	Piezoelectric (120 μm)	(External) Capacitive	[21], [22]
	Non-Cubic	Piezoelectric (160 μm)	(External) Capacitive	[23]
Figure 1.2b	Non-cubic	Magnetostrictive	Accelerometer	[24]
	Non-Cubic	Piezoelectric	Strain Gauge	[25]
	Cubic	Voice Coil	Accelerometer	[26]–[28]
	Cubic	Piezoelectric	Force	[29]
	Almost cubic	Voice Coil	Force, Accelerometer	[30], [31]
Figure 1.2c	Almost cubic	Piezoelectric	Force, Strain gauge	[32]
Figure 1.2d	Non-Cubic	3-phase rotary motor	Rotary Encoder	[33], [34]

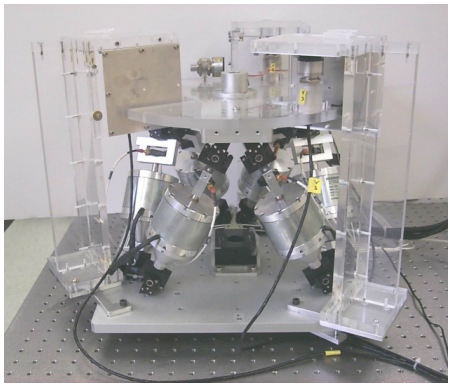

(a) Naval Postgraduate School - USA

(b) Beihang University - China

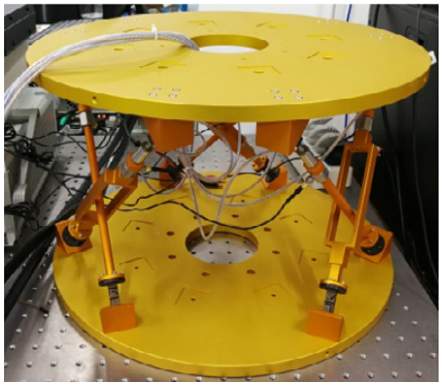

(c) Nanjing University - China

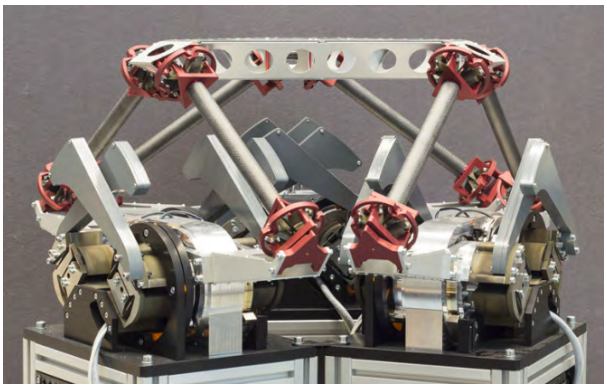

(d) University of Twente - Netherlands

Figure 1.2: Some examples of developped Stewart platform with non-cubic geometry. (a), (b), (c), (d)

  - Lot's have a "cubic" architecture that will be discussed in Section **??**
  - actuator types
  - various sensors
  - flexible joints (discussed in next chapter)
- The effect of geometry on the properties of the Stewart platform is studied in section 2
- It is determined what is the optimal geometry for the NASS

2 Effect of geometry on Stewart platform properties

- As was shown during the conceptual phase, the geometry of the Stewart platform influences:
  - the stiffness and compliance properties
  - the mobility
  - the force authority
  - the dynamics of the manipulator
- It is therefore important to understand how the geometry impact these properties, and to be able to optimize the geometry for a specific application.

One important tool to study this is the Jacobian matrix which depends on the $\boldsymbol{b}_i$ (join position w.r.t top platform) and $\hat{\boldsymbol{s}}_i$ (orientation of struts). The choice of frames ($\{A\}$ and $\{B\}$), independently of the physical Stewart platform geometry, impacts the obtained kinematics and stiffness matrix, as it is defined for forces and motion evaluated at the chosen frame.

2.1 Platform Mobility

The mobility of the Stewart platform (or any manipulator) is here defined as the range of motion that it can perform. It corresponds to the set of possible pose (i.e. combined translation and rotation) of frame {B} with respect to frame {A}. It should therefore be represented in a six dimensional space.

As was shown during the conceptual phase, for small displacements, the Jacobian matrix can be used to link the strut motion to the motion of frame B with respect to A through equation (2.1).

$$\begin{bmatrix} \delta l_1 \\ \delta l_2 \\ \delta l_3 \\ \delta l_4 \\ \delta l_5 \\ \delta l_6 \end{bmatrix} = \begin{bmatrix} {}^A\hat{\boldsymbol{s}}_1{}^T & ({}^A\boldsymbol{b}_1 \times {}^A\hat{\boldsymbol{s}}_1)^T \\ {}^A\hat{\boldsymbol{s}}_2{}^T & ({}^A\boldsymbol{b}_2 \times {}^A\hat{\boldsymbol{s}}_2)^T \\ {}^A\hat{\boldsymbol{s}}_3{}^T & ({}^A\boldsymbol{b}_3 \times {}^A\hat{\boldsymbol{s}}_3)^T \\ {}^A\hat{\boldsymbol{s}}_4{}^T & ({}^A\boldsymbol{b}_4 \times {}^A\hat{\boldsymbol{s}}_4)^T \\ {}^A\hat{\boldsymbol{s}}_5{}^T & ({}^A\boldsymbol{b}_5 \times {}^A\hat{\boldsymbol{s}}_5)^T \\ {}^A\hat{\boldsymbol{s}}_6{}^T & ({}^A\boldsymbol{b}_6 \times {}^A\hat{\boldsymbol{s}}_6)^T \end{bmatrix} \begin{bmatrix} \delta x \\ \delta y \\ \delta z \\ \delta\theta_x \\ \delta\theta_y \\ \delta\theta_z \end{bmatrix} \tag{2.1}$$

Therefore, the mobility of the Stewart platform (set of $[\delta x\ \delta y\ \delta z\ \delta\theta_x\ \delta\theta_y\ \delta\theta_z]$) depends on:

- the stroke of each strut

- the geometry of the Stewart platform (embodied in the Jacobian matrix)

More specifically:

- the XYZ mobility only depends on the si (orientation of struts)
- the mobility in rotation depends on bi (position of top joints)

As will be shown in Section **??**, there are some geometry that gives same stroke in X, Y and Z directions.

As the mobility is of dimension six, it is difficult to represent. Depending on the applications, only the translation mobility or the rotation mobility may be represented.

Mobility in translation Here, for simplicity, only translations are first considered:

- Let's consider a general Stewart platform geometry shown in Figure 2.1a.
- In the general case: the translational mobility can be represented by a 3D shape with 12 faces (each actuator limits the stroke along its orientation in positive and negative directions). The faces are therefore perpendicular to the strut direction. The obtained mobility is shown in Figure 2.1b.
- Considering an actuator stroke of $\pm d$, the mobile platform can be translated in any direction with a stroke of d A circle with radius d can be contained in the general shape. It will touch the shape along six lines defined by the strut axes. The sphere with radius d is shown in Figure 2.1b.
- Therefore, for any (small stroke) Stewart platform with actuator stroke $\pm d$, it is possible to move the top platform in any direction by at least a distance d. Note that no platform angular motion is here considered. When combining angular motion, the linear stroke decreases.
- When considering some symmetry in the system (as typically the case), the shape becomes a Trigonal trapezohedron whose height and width depends on the orientation of the struts. We only get 6 faces as usually the Stewart platform consists of 3 sets of 2 parallels struts.

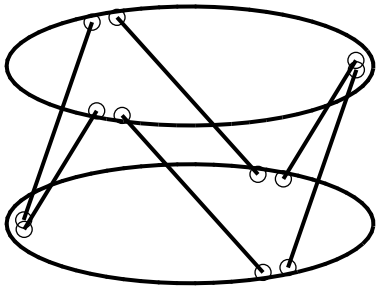

(a) Stewart platform geometry

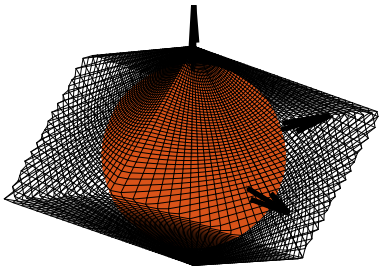

(b) Translational mobility

Figure 2.1: Example of one Stewart platform (a) and associated translational mobility (b)

To better understand how the geometry of the Stewart platform impacts the translational mobility, two configurations are compared:

- Struts oriented horizontally (Figure 2.2a) =¿ more stroke in horizontal direction
- Struts oriented vertically (Figure 2.2b) =¿ more stroke in vertical direction
- Corresponding mobility shown in Figure 2.2c

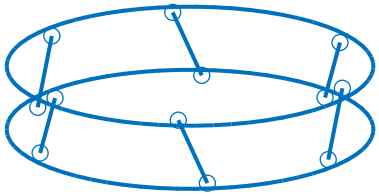

(a) Struts oriented vertically

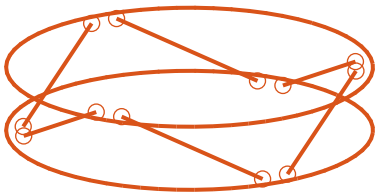

(b) Struts oriented horizontally

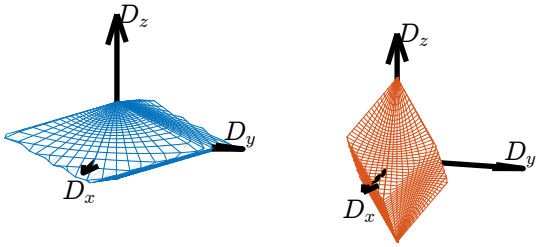

(c) Translational mobility of the two configurations

Figure 2.2: Effect of strut orientation on the obtained mobility in translation. Two Stewart platform geometry are considered: struts oriented vertically (a) and struts oriented vertically (b). Obtained mobility for both geometry are shown in (c).

Mobility in rotation As shown by equation (2.1), the rotational mobility depends both on the orientation of the struts and on the location of the top joints.

Similarly to the translational case, to increase the rotational mobility in one direction, it is advantageous to have the struts more perpendicular to the rotational direction.

For instance, having the struts more vertical (Figure 2.2a) gives less rotational stroke along the vertical direction than having the struts oriented more horizontally (Figure 2.2b).

Two cases are considered with same strut orientation but with different top joints positions:

- struts close to each other (Figure 2.3a)
- struts further apart (Figure 2.3b)

The mobility for pure rotations are compared in Figure 2.3c. Note that the same strut stroke are considered in both cases to evaluate the mobility. Having struts further apart decreases the "level arm" and therefore the rotational mobility is reduced.

For rotations and translations, having more mobility also means increasing the effect of actuator noise on the considering degree of freedom. Somehow, the level arm is increased, so any strut vibration gets amplified. Therefore, the designed Stewart platform should just have the necessary mobility.

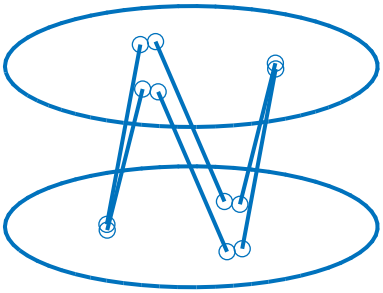

(a) Struts oriented closeically

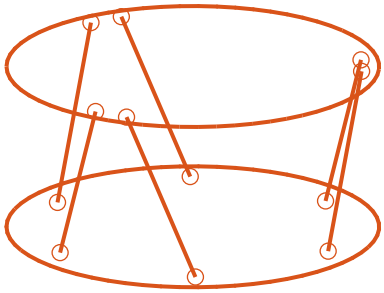

(b) Struts oriented spacezontally

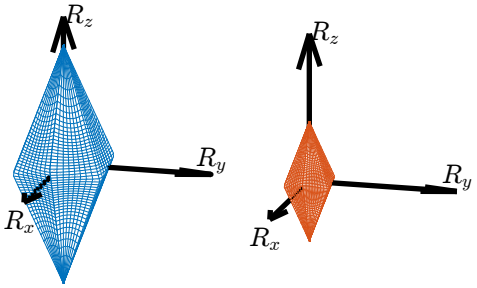

(c) Translational mobility of the two configurations

Figure 2.3: Effect of strut position on the obtained mobility in rotation. Two Stewart platform geometry are considered: struts close to each other (a) and struts further appart (b). Obtained mobility for both geometry are shown in (c).

Combined translations and rotations It is possible to consider combined translations and rotations. Displaying such mobility is more complex. It will be used for the nano-hexapod to verify that the obtained design has the necessary mobility.

For a fixed geometry and a wanted mobility (combined translations and rotations), it is possible to estimate the required minimum actuator stroke. It will be done in Section **??** to estimate the required actuator stroke for the nano-hexapod geometry.

2.2 Stiffness

Stiffness matrix:

- defines how the nano-hexapod deforms (frame $\{B\}$ with respect to frame $\{A\}$) due to static forces/torques applied on $\{B\}$.
- Depends on the Jacobian matrix (i.e. the geometry) and the strut axial stiffness (2.2)
- Contribution of joints stiffness is here not considered **mcinroy02˙model˙desig˙flexur˙joint˙stewar**, [11]

$$\boldsymbol{K} = \boldsymbol{J}^T \boldsymbol{\mathcal{K}} \boldsymbol{J} \tag{2.2}$$

It is assumed that the stiffness of all strut is the same: $\boldsymbol{\mathcal{K}} = k \cdot \mathbf{I}_6$. Obtained stiffness matrix linearly depends on the strut stiffness k (2.3).

$$\boldsymbol{K} = k\boldsymbol{J}^T\boldsymbol{J} = k \left[\begin{array}{c|c} \Sigma_{i=0}^{6} \hat{\boldsymbol{s}}_i \cdot \hat{\boldsymbol{s}}_i^T & \Sigma_{i=0}^{6} \hat{\boldsymbol{s}}_i \cdot ({}^A\boldsymbol{b}_i \times {}^A\hat{\boldsymbol{s}}_i)^T \\ \hline \Sigma_{i=0}^{6} ({}^A\boldsymbol{b}_i \times {}^A\hat{\boldsymbol{s}}_i) \cdot \hat{\boldsymbol{s}}_i^T & \Sigma_{i=0}^{6} ({}^A\boldsymbol{b}_i \times {}^A\hat{\boldsymbol{s}}_i) \cdot ({}^A\boldsymbol{b}_i \times {}^A\hat{\boldsymbol{s}}_i)^T \end{array} \right] \tag{2.3}$$

Translation Stiffness XYZ stiffnesses:

- Only depends on the orientation of the struts and not their location: $\hat{\boldsymbol{s}}_i \cdot \hat{\boldsymbol{s}}_i^T$
- Extreme case: all struts are vertical $s_i = [0,\ 0,\ 1]$ =¿ vertical stiffness of $6k$, but null stiffness in X and Y directions
- If two struts along X, two struts along Y, and two struts along Z =¿ $\hat{\boldsymbol{s}}_i \cdot \hat{\boldsymbol{s}}_i^T = 2\boldsymbol{I}_3$ Stiffness is well distributed along directions. This corresponds to the cubic architecture.

If struts more vertical (Figure 2.2a):

- increase vertical stiffness
- decrease horizontal stiffness
- increase Rx,Ry stiffness
- decrease Rz stiffness

Opposite conclusions if struts are not horizontal (Figure 2.2b).

Rotational Stiffness Rotational stiffnesses:

- Same orientation but increased distances (bi) by a factor 2 =¿ rotational stiffness increased by factor 4 Figure 2.3a Figure 2.3b

Struts further apart:

- no change to XYZ
- increase in rotational stiffness (by the square of the distance)

Diagonal Stiffness Matrix

2.3 Dynamics ?

Dynamical equations (both in the cartesian frame and in the frame of the struts) for the Stewart platform were derived during the conceptual phase with simplifying assumptions (massless struts and perfect joints). The dynamics depends both on the geometry (Jacobian matrix) but also on the payload being placed on top of the platform.

Under very specific conditions, the equations of motion can be decoupled in the Cartesian space. These are studied in Section **??**.

$$\frac{\mathcal{X}}{\mathcal{F}}(s) = (\boldsymbol{M}s^2 + \boldsymbol{J}^T\boldsymbol{\mathcal{C}}\boldsymbol{J}s + \boldsymbol{J}^T\boldsymbol{\mathcal{K}}\boldsymbol{J})^{-1} \tag{2.4}$$

In the frame of the struts, the equations of motion are well decoupled at low frequency. This is why most of Stewart platforms are controlled in the frame of the struts: bellow the resonance frequency, the system is decoupled and SISO control may be applied for each strut.

$$\frac{\mathcal{L}}{\mathcal{f}}(s) = (\boldsymbol{J}^{-T}\boldsymbol{M}\boldsymbol{J}^{-1}s^2 + \boldsymbol{\mathcal{C}} + \boldsymbol{\mathcal{K}})^{-1} \tag{2.5}$$

For the NASS, the payloads can have various inertia, with masses ranging from 1 to 50kg. It is therefore not possible to have one geometry that gives good dynamical properties for all the payloads.

Coupling between force sensors in different struts may also be important.

- ☐ Maybe study that for the cubic architecture, and then say that except for very specific conditions, coupling is similar for different geometries

Conclusion

The effects of two changes in the manipulator's geometry, namely the position and orientation of the legs, are summarized in Table 2.1. These results could have been easily deduced based on some mechanical principles, but thanks to the kinematic analysis, they can be quantified.

These trade-offs give some guidelines when choosing the Stewart platform geometry.

Table 2.1: Effect of a change in geometry on the manipulator's stiffness, force authority and stroke

	legs pointing more vertically	**legs further apart**
Vertical stiffness	$\nearrow$	$=$
Horizontal stiffness	$\searrow$	$=$
Vertical rotation stiffness	$\searrow$	$\nearrow$
Horizontal rotation stiffness	$\nearrow$	$\nearrow$
Vertical force authority	$\nearrow$	$=$
Horizontal force authority	$\searrow$	$=$
Vertical torque authority	$\searrow$	$\nearrow$
Horizontal torque authority	$\nearrow$	$\nearrow$
Vertical stroke	$\searrow$	$=$
Horizontal stroke	$\nearrow$	$=$
Vertical rotation stroke	$\nearrow$	$\searrow$
Horizontal rotation stroke	$\searrow$	$\searrow$

3 Conclusion

Inertia used for experiments will be very broad =¿ difficult to optimize the dynamics Specific geometry is not found to have a huge impact on performances. Practical implementation is important.

Geometry impacts the static and dynamical characteristics of the Stewart platform. Considering the design constrains, the slight change of geometry will not significantly impact the obtained results.

Bibliography

[1] Z. Geng and L. S. Haynes, "Six-degree-of-freedom active vibration isolation using a stewart platform mechanism," *Journal of Robotic Systems*, vol. 10, no. 5, pp. 725–744, 1993 (cit. on p. 5).

[2] Z. Geng and L. Haynes, "Six degree-of-freedom active vibration control using the stewart platforms," *IEEE Transactions on Control Systems Technology*, vol. 2, no. 1, pp. 45–53, 1994 (cit. on p. 5).

[3] Z. J. Geng, G. G. Pan, L. S. Haynes, B. K. Wada, and J. A. Garba, "An intelligent control system for multiple degree-of-freedom vibration isolation," *Journal of Intelligent Material Systems and Structures*, vol. 6, no. 6, pp. 787–800, 1995 (cit. on p. 5).

[4] J. Spanos, Z. Rahman, and G. Blackwood, "A soft 6-axis active vibration isolator," in *Proceedings of 1995 American Control Conference - ACC'95*, 1995 (cit. on p. 5).

[5] Z. H. Rahman, J. T. Spanos, and R. A. Laskin, "Multiaxis vibration isolation, suppression, and steering system for space observational applications," in *Telescope Control Systems III*, May 1998 (cit. on p. 5).

[6] D. Thayer and J. Vagners, "A look at the pole/zero structure of a stewart platform using special coordinate basis," in *Proceedings of the 1998 American Control Conference. ACC (IEEE Cat. No.98CH36207)*, 1998 (cit. on p. 5).

[7] D. Thayer, M. Campbell, J. Vagners, and A. von Flotow, "Six-axis vibration isolation system using soft actuators and multiple sensors," *Journal of Spacecraft and Rockets*, vol. 39, no. 2, pp. 206–212, 2002 (cit. on p. 5).

[8] G. Hauge and M. Campbell, "Sensors and control of a space-based six-axis vibration isolation system," *Journal of Sound and Vibration*, vol. 269, no. 3-5, pp. 913–931, 2004 (cit. on p. 5).

[9] J. McInroy, "Dynamic modeling of flexure jointed hexapods for control purposes," in *Proceedings of the 1999 IEEE International Conference on Control Applications (Cat. No.99CH36328)*, 1999 (cit. on p. 5).

[10] J. McInroy, J. O'Brien, and G. Neat, "Precise, fault-tolerant pointing using a stewart platform," *IEEE/ASME Transactions on Mechatronics*, vol. 4, no. 1, pp. 91–95, 1999 (cit. on p. 5).

[11] J. McInroy and J. Hamann, "Design and control of flexure jointed hexapods," *IEEE Transactions on Robotics and Automation*, vol. 16, no. 4, pp. 372–381, 2000 (cit. on pp. 5, 12).

[12] X. Li, J. C. Hamann, and J. E. McInroy, "Simultaneous vibration isolation and pointing control of flexure jointed hexapods," in *Smart Structures and Materials 2001: Smart Structures and Integrated Systems*, Aug. 2001 (cit. on p. 5).

[13] F. Jafari and J. McInroy, "Orthogonal gough-stewart platforms for micromanipulation," *IEEE Transactions on Robotics and Automation*, vol. 19, no. 4, pp. 595–603, Aug. 2003 (cit. on p. 5).

[14] A. Defendini, L. Vaillon, F. Trouve, *et al.*, "Technology predevelopment for active control of vibration and very high accuracy pointing systems," in *Spacecraft Guidance, Navigation and Control Systems*, vol. 425, 2000, p. 385 (cit. on p. 5).

[15] A. Abu Hanieh, M. Horodinca, and A. Preumont, "Stiff and soft stewart platforms for active damping and active isolation of vibrations," in *Actuator 2002, 8th International Conference on New Actuators*, 2002 (cit. on p. 5).

[16] H.-J. Chen, R. Bishop, and B. Agrawal, "Payload pointing and active vibration isolation using hexapod platforms," in *44th AIAA/ASME/ASCE/AHS/ASC Structures, Structural Dynamics, and Materials Conference*, Apr. 2003 (cit. on p. 5).

[17] A. A. Hanieh, "Active isolation and damping of vibrations via stewart platform," Ph.D. dissertation, Université Libre de Bruxelles, Brussels, Belgium, 2003 (cit. on p. 5).

[18] A. Preumont, M. Horodinca, I. Romanescu, *et al.*, "A six-axis single-stage active vibration isolator based on stewart platform," *Journal of Sound and Vibration*, vol. 300, no. 3-5, pp. 644–661, 2007 (cit. on p. 5).

[19] B. N. Agrawal and H.-J. Chen, "Algorithms for active vibration isolation on spacecraft using a stewart platform," *Smart Materials and Structures*, vol. 13, no. 4, pp. 873–880, 2004 (cit. on p. 5).

[20] K. Furutani, M. Suzuki, and R. Kudoh, "Nanometre-cutting machine using a stewart-platform parallel mechanism," *Measurement Science and Technology*, vol. 15, no. 2, pp. 467–474, 2004 (cit. on p. 5).

[21] Y. Ting, H.-C. Jar, and C.-C. Li, "Design of a 6dof stewart-type nanoscale platform," in *2006 Sixth IEEE Conference on Nanotechnology*, 2006 (cit. on p. 5).

[22] Y. Ting, C.-C. Li, and T. V. Nguyen, "Composite controller design for a 6dof stewart nanoscale platform," *Precision Engineering*, vol. 37, no. 3, pp. 671–683, 2013 (cit. on p. 5).

[23] Y. Ting, H.-C. Jar, and C.-C. Li, "Measurement and calibration for stewart micromanipulation system," *Precision Engineering*, vol. 31, no. 3, pp. 226–233, 2007 (cit. on p. 5).

[24] Z. Zhang, J. Liu, J. Mao, Y. Guo, and Y. Ma, "Six dof active vibration control using stewart platform with non-cubic configuration," in *2011 6th IEEE Conference on Industrial Electronics and Applications*, Jun. 2011 (cit. on p. 5).

[25] Z. Du, R. Shi, and W. Dong, "A piezo-actuated high-precision flexible parallel pointing mechanism: Conceptual design, development, and experiments," *IEEE Transactions on Robotics*, vol. 30, no. 1, pp. 131–137, 2014 (cit. on p. 5).

[26] W. Chi, D. Cao, D. Wang, *et al.*, "Design and experimental study of a vcm-based stewart parallel mechanism used for active vibration isolation," *Energies*, vol. 8, no. 8, pp. 8001–8019, 2015 (cit. on p. 5).

[27] J. Tang, D. Cao, and T. Yu, "Decentralized vibration control of a voice coil motor-based stewart parallel mechanism: Simulation and experiments," *Proceedings of the Institution of Mechanical Engineers, Part C: Journal of Mechanical Engineering Science*, vol. 233, no. 1, pp. 132–145, 2018 (cit. on p. 5).

[28] J. Jiao, Y. Wu, K. Yu, and R. Zhao, "Dynamic modeling and experimental analyses of stewart platform with flexible hinges," *Journal of Vibration and Control*, vol. 25, no. 1, pp. 151–171, 2018 (cit. on p. 5).

[29] C. Wang, X. Xie, Y. Chen, and Z. Zhang, "Investigation on active vibration isolation of a stewart platform with piezoelectric actuators," *Journal of Sound and Vibration*, vol. 383, pp. 1–19, Nov. 2016 (cit. on p. 5).

[30] M. Beijen, M. Heertjes, J. V. Dijk, and W. Hakvoort, "Self-tuning mimo disturbance feedforward control for active hard-mounted vibration isolators," *Control Engineering Practice*, vol. 72, pp. 90–103, 2018 (cit. on p. 5).

[31] D. Tjepkema, "Active hard mount vibration isolation for precision equipment [ph. d. thesis]," Ph.D. dissertation, 2012 (cit. on p. 5).

[32] X. Yang, H. Wu, B. Chen, S. Kang, and S. Cheng, "Dynamic modeling and decoupled control of a flexible stewart platform for vibration isolation," *Journal of Sound and Vibration*, vol. 439, pp. 398–412, Jan. 2019 (cit. on p. 5).

[33] M. Naves, "Design and optimization of large stroke flexure mechanisms," Ph.D. dissertation, Univeristy of Twente, 2020 (cit. on p. 5).

[34] M. Naves, W. Hakvoort, M. Nijenhuis, and D. Brouwer, "T-flex: A large range of motion fully flexure-based 6-dof hexapod," in *20th EUSPEN International Conference & Exhibition, EUSPEN 2020*, EUSPEN, 2020, pp. 205–208 (cit. on p. 5).